ChemComm

Accepted Manuscript

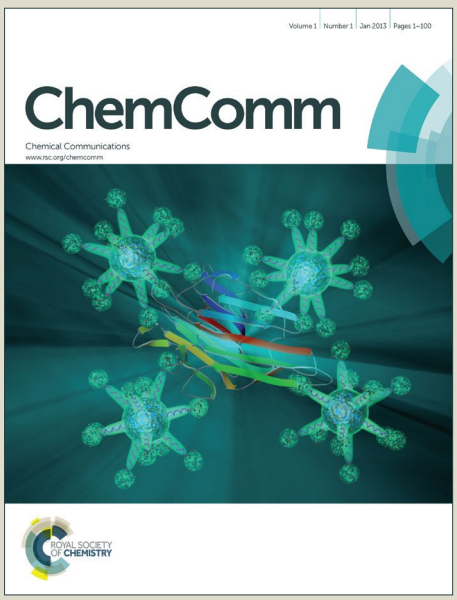




ROYAL SOCIETY OF CHEMISTRY

www.rsc.org/chemcomm

ChemComm

COMMUNICATION

# Superior catalytic activity derived from two-dimensional $Ti_3C_2$ precursor towards the hydrogen storage reaction of magnesium hydride†

Received 00th January 20xx,
Accepted 00th January 20xx

DOI: 10.1039/x0xx00000x

www.rsc.org/chemcomm

Yongfeng Liu[a,b], Hufei Du[a], Xin Zhang[a], Yaxiong Yang,[a] Mingxia Gao[a], Hongge Pan[a,*]

**The superior catalytic effects derived from a 2D $Ti_3C_2$ (MXene), synthesized by the exfoliation of $Ti_3AlC_2$ powders, towards the hydrogen storage reaction of $MgH_2$ were demonstrated. The 5 wt% $Ti_3C_2$-containing $MgH_2$ releases 6.2 wt% $H_2$ within 1 min at 300 °C and absorbs 6.1 wt% $H_2$ within 30 s at 150 °C, exhibiting excellent dehydrogenation/hydrogenation kinetics.**

Magnesium hydride ($MgH_2$) has attracted intense interest as one of the most promising candidates for reversible hydrogen storage because of its high hydrogen capacity (7.6 wt%), good reversibility and low cost.[1] Unfortunately, reversible hydrogen storage with $MgH_2$ suffers from high operating temperatures and sluggish reaction kinetics that severely hinders its practical utilization, especially for mobile applications. Over the past few decades, numerous efforts have been devoted to overcoming these barriers through alloying, catalysing and nanostructuring.[2-4] It has been proven that the introduction of catalysts, including transition metals (*i.e.* Ti, Nb, V, Co, Mo, Fe, Mn, Ni and Ce) and their compounds, to $MgH_2$ is quite effective in reducing the operating temperature and enhancing the reaction kinetics of hydrogen storage.[3,5] Among these developed catalysts, Ti-based compounds have been found to possess very high activity.[6-9] Cui et al.[7] designed a multi valent Ti-containing Mg composite that starts releasing $H_2$ at approximately 175 °C, and the hydrogen release amounts to 5 wt% within 15 min at 250 °C. Shao et al.[8] reported that $TiH_2$ is also a good catalytic additive to improve the hydrogen storage kinetics of $MgH_2$. Anastasopol et al.[9] successfully synthesized Mg-Ti nanoparticles by spark discharge generation that show a distinct reduction in the enthalpy of formation for hydride (−45 ± 3 kJ $mol^{-1}$). In addition to Ti-based species, nanoscaled metal-carbon composites are also a widely studied class of additives for further enhancement of the hydrogen sorption kinetics of $MgH_2$.[10-13] Liu et al.[11] disclosed that the porous 5 wt% Ni@rGO-containing $MgH_2$ rapidly desorbs 6.0 wt% $H_2$ within 10 min at 300 °C. Wang et al.[12] reported that a 10 wt% TiN@rGO-doped $MgH_2$ sample begins releasing hydrogen at approximately 167 °C, and 6.0 wt% hydrogen is released within 18 min, when isothermally heated at 300 °C. More encouragingly, Tan and co-workers[13] demonstrated that the $Mg_{95}Ni_5$-$TiO_2$/MWCNT system absorbed 5.6 wt% $H_2$ within 60 s at 100 °C and released 6.08 wt% $H_2$ within 600 s at 280 °C. The synergetic effects of metallic nanoparticles and carbon are believed to be responsible for the high catalytic activities of nanoscaled metal-carbon composites, which improve the hydrogen storage properties of $MgH_2$.[10-13]

Recently, MXenes, a new class of 2D early-transition-metal carbides, have been successfully synthesized by exfoliation of ternary carbides, nitrides, or carbonitrides (MAX phase).[14,15] The exfoliation process uses HF to selectively etch the A layers from the MAX phase and is accompanied by the surface replacement of OH and F groups. MXenes with a particular layered structure show promise for use as an anode material for Li-ion batteries.[16] Considerations based on the similarity between MXenes and metal-carbon nanostructure composites reasonably suggest that the 2D $Ti_3C_2$ could possess superior catalytic activity towards the hydrogen storage reaction of $MgH_2$. Herein, we conduct the first attempt to promote the catalytic function of 2D $Ti_3C_2$ as a novel catalyst precursor for the reversible hydrogen storage behaviours of $MgH_2$.

The layered $Ti_3C_2$ was synthesized by the exfoliation of $Ti_3AlC_2$ with an HF solution for 72 h at room temperature. XRD (Fig. 1) proved the formation of $Ti_3C_2$, which was accomplished by selectively removing Al from $Ti_3AlC_2$, through the disappearance of the strongest diffraction peak of $Ti_3AlC_2$ at $2\vartheta$ = 39° and the shift of the (002) and (004) peaks to lower angles.[14] SEM observations indicated that the $Ti_3C_2$ basal

[a] *State Key Laboratory of Silicon Materials, Key Laboratory of Advanced Materials and Applications for Batteries of Zhejiang Province and School of Materials Science and Engineering, Zhejiang University, Hangzhou 310027, China. E-mail: mselyf@zju.edu.cn, Fax: +86-571-87952615*

[b] *Key Laboratory of Advanced Energy Materials Chemistry (Ministry of Education), Nankai University, Tianjin 300071, China*

†Electronic supplementary information (ESI) available: Material preparation and characterization; comparison of de-/hydrogenation kinetics of $MgH_2$ with various Ti-based catalysts; EDS of as-prepared $Ti_3C_2$; Isothermal de-/hydrogenation curves of pristine $MgH_2$; cycling performance of $MgH_2$-5 wt% $Ti_3C_2$; Kissinger plots of $MgH_2$ and $MgH_2$-5 wt% $Ti_3C_2$; XRD of as-milled $MgH_2$-20 wt% $Ti_3C_2$; SEM image and EDS of $MgH_2$-5 wt% $Ti_3C_2$. See DOI: 10.1039/x0xx00000x

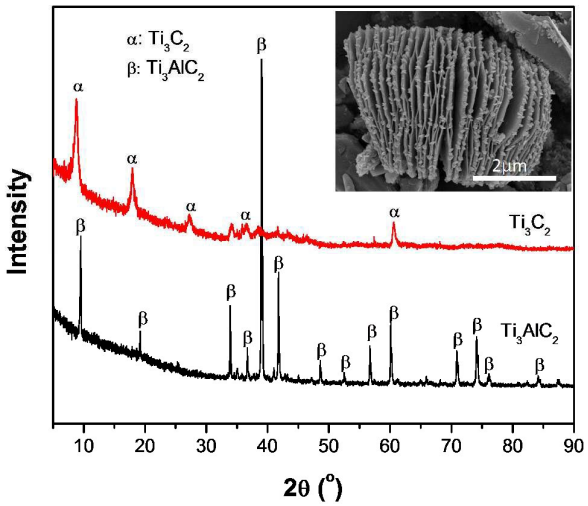


Fig. 1 XRD patterns of $Ti_3AlC_2$ and as-prepared $Ti_3C_2$. The inset is an SEM image of $Ti_3C_2$.

planes were effectively separated following the HF treatment and exhibit a multilayer morphology, as shown in the inset of Fig. 1. EDS analysis further revealed that the resultant product was composed mainly of Ti and C and contained a small amount of O and F, which is attributed to the replacement of Al layers with OH and/or F (Fig. S1, ESI†).

The as-prepared layered $Ti_3C_2$ was used as a catalyst precursor to improve the hydrogen storage properties of $MgH_2$. Five samples of $MgH_2$-*x* wt% $Ti_3C_2$ (*x* = 0, 1, 3, 5 and 7) were prepared by ball milling under 50 bar hydrogen for 24 h. Fig. 2a shows the volumetric release curves of the as-prepared $MgH_2$-*x* wt% $Ti_3C_2$ samples. As expected, adding small amounts of $Ti_3C_2$ significantly lowered the dehydrogenation temperatures with respect to $MgH_2$. The operating temperature for the rapid dehydrogenation of the $MgH_2$-5 wt% $Ti_3C_2$ composite was reduced from 278 °C (pristine $MgH_2$) to 185 °C, representing a 93 °C reduction. Further increasing the $Ti_3C_2$ content to 7 wt% caused the onset dehydrogenation temperature to decline slightly to 180 °C. Meanwhile, an approximately 3% decrease in the dehydrogenation capacity, from 7.2 wt% to 7.0 wt%, was also observed because of the dead weight of $Ti_3C_2$. When considering the observed effects to both the operating temperature and the hydrogen capacity, it is suggested that $MgH_2$-5 wt% $Ti_3C_2$ represents the optimal concentration. This configuration released approximately 7.1 wt% hydrogen with an onset temperature of 185 °C and a terminal temperature of 350 °C, upon dynamic heating. Further isothermal measurements presented remarkably enhanced kinetics for the release of hydrogen from the $MgH_2$-5 wt% $Ti_3C_2$ sample. As shown in Fig. 2b, the $MgH_2$-5 wt% $Ti_3C_2$ sample liberated approximately 5.0 wt% hydrogen within 10 min at 250 °C. However, no appreciable hydrogen release was detected for the pristine $MgH_2$ under identical conditions (Fig. S2, ESI†). When hydrogen desorption was performed at 300 °C, the $MgH_2$-5 wt% $Ti_3C_2$ sample released approximately 6.2 wt% hydrogen within only 1 min, while more than 80 min was required for pristine $MgH_2$ to release the same amount. Therefore, the dehydrogenation rate of $MgH_2$ is significantly improved (ca. 80 times faster) by the presence of the 2D $Ti_3C_2$.

The effects of $Ti_3C_2$ on the hydrogen storage reversibility of $MgH_2$ were further evaluated by hydriding the fully dehydrogenated sample under 50 bar hydrogen pressure. Fig. 3a shows the non-isothermal hydrogenation curves for the dehydrogenated pristine $MgH_2$ and $MgH_2$-5 wt% $Ti_3C_2$ samples. It was observed that the dehydrogenated $MgH_2$-5 wt% $Ti_3C_2$ sample began absorbing hydrogen at room temperature, and the hydrogen uptake amounted to 5.5 wt% at 100 °C, which is distinctly superior to the uptake of pristine $MgH_2$ (< 1 wt%). While heating to 180 °C, approximately 6.7 wt% hydrogen was added to the $MgH_2$-5 wt% $Ti_3C_2$ complex, which exhibited good reversibility. The isothermal hydrogenation experiments showed that the dehydrogenated $MgH_2$-5 wt% $Ti_3C_2$ sample absorbed approximately 3.0 wt% hydrogen within 150 s at temperatures as low as 50 °C (Fig. 3b). However, under identical conditions, less than 0.5 wt% hydrogen was taken up

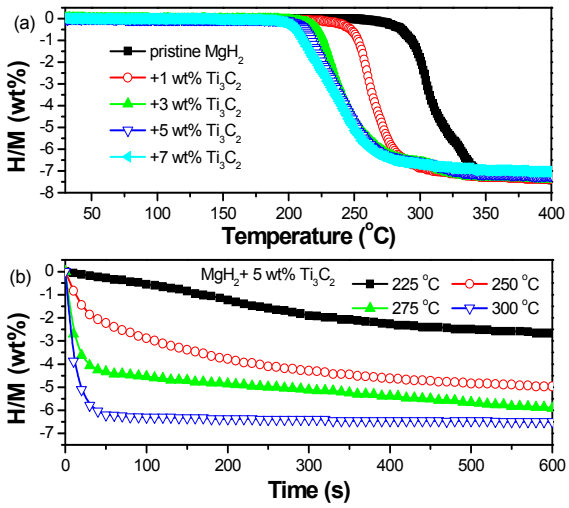


Fig. 2 Non-isothermal (a) and isothermal (b) dehydrogenation curves of the $MgH_2$-*x* wt% $Ti_3C_2$ samples.

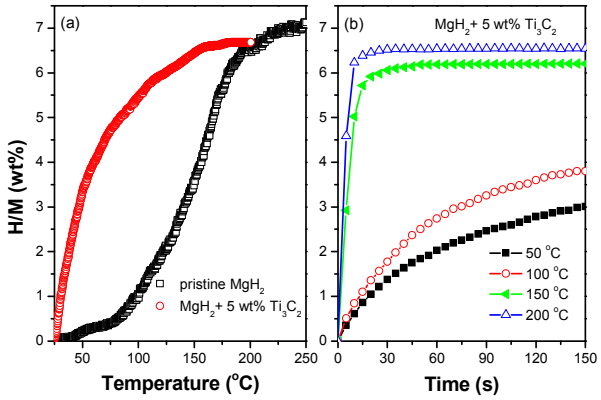


Fig. 3 Non-isothermal (a) and isothermal (b) hydrogenation curves of the dehydrogenated $MgH_2$-*x* wt% $Ti_3C_2$ samples.

by the dehydrogenated pristine $MgH_2$ (Fig. S3, ESI†). At 150 °C, the dehydrogenated $MgH_2$-5 wt% $Ti_3C_2$ sample could take up 6.1 wt% hydrogen within 30 s, whereas only 4.2 wt% was stored by the dehydrogenated $MgH_2$ sample, even when the dwell time was extended to 2000 s. By analysing the tangent slope of the linear region of the hydrogen uptake at 150 °C, the rate constant for $MgH_2$-5 wt% $Ti_3C_2$ was estimated as 23.09 wt% $min^{-1}$, which is approximately 115 times greater than that of the pristine $MgH_2$ sample (0.20 wt% $min^{-1}$). Apparently, the presence of $Ti_3C_2$ is also quite beneficial to the $MgH_2$ hydrogen absorption process. Further cycling measurements exhibited good stability over the first 10 cycles with a 6.4 wt% reversible capacity (> 95% capacity retention) for the $MgH_2$-5 wt% $Ti_3C_2$ composite (Fig. S4, ESI†). More importantly, the catalytic efficiency of $Ti_3C_2$ in enhancing the dehydrogenation/hydrogenation kinetics of $MgH_2$ exceeds most of the currently known Ti-based materials, as shown in Table S1 (ESI†).[10,12,17] The apparent activation energy ($E_a$) was calculated as 98.9 kJ $mol^{-1}$ for the release of hydrogen from the $MgH_2$-5 wt% $Ti_3C_2$ composite, which is a 36% reduction relative to that of the pristine $MgH_2$ (155.1 kJ $mol^{-1}$) (Fig. S5, ESI†). This explains the significantly reduced dehydrogenation temperatures and favourable dehydrogenation kinetics and is possibly attributable to the unique layered structure of $Ti_3C_2$.

To understand the role played by $Ti_3C_2$ during the dehydrogenation chemical process, the structures and morphologies of composite samples were examined by XRD, SEM and XPS. $MgH_2$-5 wt% $Ti_3C_2$ samples were collected after ball milling and after full dehydrogenation. As shown in Fig. 4(a), the XRD profile of the as-milled $MgH_2$-5 wt% $Ti_3C_2$ composite displays reflections typical of $\beta$-$MgH_2$. Moreover, the MgO phase was also identified; its dominant peak was visible at $2\vartheta$ = 42.8°. It is possible that this phase originated from the reaction between $MgH_2$ and the –OH that is distributed on the surface of $Ti_3C_2$ after washing, as seen in Fig. S1 (ESI†). However, it is noteworthy that no Ti- and C-containing phases were detected by XRD, even when the level of $Ti_3C_2$ was increased to 20 wt% (Fig. S6, ESI†). This phenomenon is likely due to the poor crystallization of $Ti_3C_2$ and/or a chemical reaction between $Ti_3C_2$ and the $MgH_2$ matrix. To reveal the existing state of $Ti_3C_2$, EDS and XPS analyses were further conducted, and the results are presented in Fig. 4(b-d). EDS mapping results (Fig. 4(b)) display a relatively homogeneous distribution of Ti and C in the $Ti_3C_2$-containing $MgH_2$ sample, which remains nearly unchanged after dehydrogenation (Fig. S7, ESI†). As shown in Fig. 4(c), XPS peak fitting indicates that the Ti 2p spectrum of pristine $Ti_3C_2$ can be resolved into four sets of $2p_{3/2}$-$2p_{1/2}$ spin-orbit doublets at 454.6/460.3 eV, 456.4/461.5 eV, 457.0/462.4 eV and 458.8/464.4 eV that correspond to Ti-C, $Ti^{2+}$, $Ti^{3+}$ and $TiO_2$, respectively.[18] A small amount of $TiO_2$ is likely originated from the reaction between $Ti_3C_2$ and the –OH caused by the local heat generated during HF treatment of MAX phase as reported previously.[19] After ball-milling $Ti_3C_2$ with $MgH_2$, only the peaks assignable to $Ti^0$ (453.7/459.8 eV)[20] and $Ti^{2+}$ (456.4/461.5 eV) were observed along with the disappearance of the peaks of Ti-C, $Ti^{3+}$ and $TiO_2$. Meanwhile, the absence of Ti-C peaks was also identified in high-resolution C 1s XPS spectrum of $Ti_3C_2$-containing $MgH_2$ sample after ball milling.[21] Here, the appearance of the $Ti^0$ peaks indicates that the $Ti_3C_2$ was reduced to metallic Ti during ball milling. The *in situ* formed metallic Ti facilitates the dissociation and recombination of molecular hydrogen on its surface, consequently improving the dehydrogenation kinetics of $MgH_2$ as has been reported previously.[22]

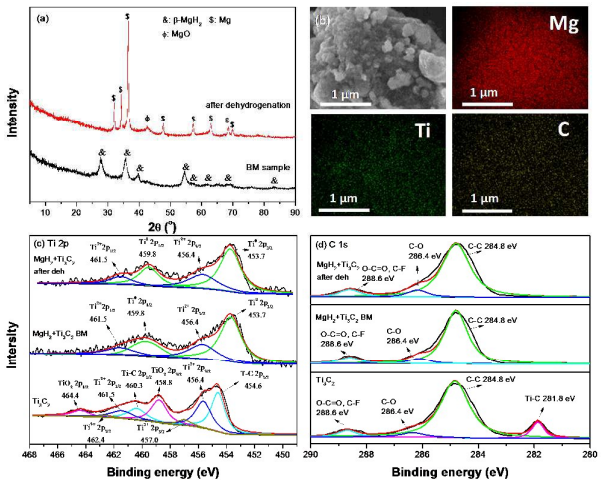


Fig. 4 (a) XRD patterns of the $MgH_2$-5 wt% $Ti_3C_2$ sample before and after dehydrogenation, (b) EDS mapping results of the as-milled $MgH_2$-5 wt% $Ti_3C_2$ sample, and (c, d) Ti 2p and C 1s XPS spectra of $Ti_3C_2$ and $Ti_3C_2$-containing $MgH_2$ samples at different states.

After dehydrogenation, the hexagonal Mg phase was unambiguously identified in the XRD profile (Fig. 4(a)), along with an absence of the $\beta$-$MgH_2$ phase. XPS results exhibited a quite identical spectrum to that of the as-milled sample (Fig. 4(c)), representing the preservation of the metallic Ti and $Ti^{2+}$ states in the dehydrogenated product, that is, the metallic Ti and $Ti^{2+}$ keep stable during dehydrogenation. Moreover, SEM revealed distinctly reduced particle sizes for the $MgH_2$-5 wt% $Ti_3C_2$ composite after 10 uptake/release cycles (Fig. S8), which is indicative of a pulverization process. This observation explains the progressive decrease in the onset of the dehydrogenation temperature for $MgH_2$-5 wt% $Ti_3C_2$ with cycling, as shown in Fig. S4(b) (ESI†).

In summary, the 2D $Ti_3C_2$ (MXene) synthesized by the exfoliation of the MAX phase of $Ti_3AlC_2$ exhibited superior catalytic effects as a catalyst precursor towards the hydrogen storage reaction of $MgH_2$. The onset of the dehydrogenation temperature for the $MgH_2$-5 wt% $Ti_3C_2$ sample was 185 °C, which marks a 93 °C reduction relative to the pristine sample. At 300 °C, approximately 6.2 wt% $H_2$ rapidly evolved from the $MgH_2$-5 wt% $Ti_3C_2$ composite within 1 min of heating. More importantly, the dehydrogenated sample initiated hydrogen absorption at room temperature, and the hydrogen uptake reached 6.1 wt% $H_2$ within 30 s at 150 °C. The dehydrogenation/hydrogenation kinetics of the $Ti_3C_2$-containing $MgH_2$ are superior to those samples doped with other Ti-based materials. The unique layered structure and the *in situ* formed metallic Ti are likely the most important reasons

for the high catalytic activity of $Ti_3C_2$, which manifests in a reduction of the operating temperature and an enhancement of the reaction kinetics for hydrogen storage in $MgH_2$.

We gratefully acknowledge financial support received from the National Natural Science Foundation of China (51222101, 51171170), the Research Fund for the Doctoral Program of Higher Education of China (20130101110080, 20130101130007), Zhejiang Provincial Natural Science Foundation of China (LR16E010002) and from the Fundamental Research Funds for the Central Universities (2014XZZX003-08, 2014XZZX005).

## Notes and references

1 B. Peng, J. Liang, Z. L. Tao and J. Chen, *J. Mater. Chem.*, 2009, **19**, 2877-2883; K. F. Aguey-Zinsou and J. R. Ares-Fernández, *Energy Environ. Sci.*, 2010, **3**, 526-543; I. P. Jain, C. Lal and A. Jain, *Int. J. Hydrogen Energy*, 2010, **35**, 5133-5144; F. Schüth, B. Bogdanović and M. Felderhoff, *Chem. Commun.*, 2004, **20**, 2249-2258.

2 M. Zhu, Y. S. Lu, L. Z. Ouyang and H. Wang, *Materials*, 2013, **6**, 4654-4674; J. Huot, G. Liang and R. Schulz, *Appl. Phys. A*, 2001, **72**, 187-195; S. Orimo and H. Fujii, *Appl. Phys. A*, 2001, **72**, 167-186; E. Akiba, *Curr. Opin. Solid State Mater. Sci.*, 1999, **4**, 267-272; B. Sakintunaa, F. Lamari-Darkrimb and M. Hirscher, *Int. J. Hydrogen Energy*, 2007, **32**, 1121-1140.

3 C. J. Webb, *J. Phys. Chem. Solids*, 2015, **84**, 96–106; N. Bazzanella, R. Checchetto and A. Miotello, *J. Nanomterials*, 2011, **2011**, 1-11; R. A. Varin, L. Zbroniec, M. Polanski and J. Bystrzycki, *Energies*, 2011, **4**, 1-25.

4 H. Y. Shao, G. B. Xin, J. Zheng, X. G. Li and E. Akiba, *Nano Energy*, 2012, **1**, 590-601; Y. Jia, C. H. Sun, S. H. Shen, J. Zou, S. S. Mao and X. D. Yao, *Renewable Sustainable Energy Rev.*, 2015, **44**, 289-303; P. E. de Jongh and P. Adelhelm, *ChemSusChem*, 2010, **3**, 1332-1348; T. K. Nielsen, F. Besenbacher and T. R. Jensen, *Nanoscale*, 2011, **3**, 2086-2098; W. Y. Li, C. S. Li, H. Ma and J. Chen, *J. Am. Chem. Soc.*, 2007, **129**, 6710-6711; F. Y. Cheng, Z. L. Tao, J. Liang and J. Chen, *Chem. Commun.*, 2012, **48**, 7334-7343; Y. S. Au, M. K. Obbink, S. Srinivasan, P. C. M. M. Magusin, K. P. de Jong and P. E. de Jongh, *Adv. Funct. Mater.*, 2014, **24**, 3604-3611.

5 M. Ismail, *Int. J. Hydrogen Energy*, 2014, **39**, 2567-2574; J. Cui, J. W. Liu, H. Wang, L. Z. Ouyang, D. L. Sun, M. Zhu and X. D. Yao, *J. Mater. Chem. A*, 2014, **2**, 9645-9655; J. G. Yuan, Y. F. Zhu and L. Q. Li, *Chem. Commun.*, 2014, **50**, 6641-6644; L. Z. Ouyang, J. J. Tang, Y. J. Zhao, H. Wang, X. D. Yao, J. W. Liu, J. Zou and M. Zhu, *Sci. Rep.*, 2015, **5**, 10776.

6 M. Y. Song, S. N. Kwon, H. R. Park and J. L. Bobet, *Int. J. Hydrogen Energy*, 2011, **36**, 12932-12938; N. Mahmoudi, A. Kaflou and A. Simchi, *Mater. Lett.*, 2011, **65**, 1120-1122; P. Vermeulen, E. F. M. J. van Thiel and P. H. L. Notten, *Chem.-Eur. J.*, 2007, **13**, 9892-9898; J. Lu, Y. J. Choi, Z. Z. Fang, H. Y. Sohn and E. Rönnebro, *J. Am. Chem. Soc.*, 2009, **131**, 15843-15852.

7 J. Cui, H. Wang, J. W. Liu, L. Z. Ouyang, Q. G. Zhang, D. L. Sun, X. D. Yao and M. Zhu, *J. Mater. Chem. A*, 2013, **1**, 5603-5611.

8 H. Shao, M. Felderhoff, F. Schüth and C. Weidenthaler, *Nanotechnology,* 2011, **22**, 235401.

9 A. Anastasopol, T. V. Pfeiffer, J. Middelkoop, U. Lafont, R. J. Canales-Perez, A. Schmidt-Ott, F. M. Mulder and S. W. H. Eijt, *J. Am. Chem. Soc.*, 2013, **135**, 7891-7900.

10 Y. Jia, L. Cheng, N. Pan, J. Zou, G. Q. Lu and X. D. Yao, *Adv. Energy Mater.*, 2011, **1**, 387-393; X. D. Yao, C. Z. Wu, A. J. Du, J. Zou, Z. H. Zhu, P. Wang, H. M. Cheng, S. Smith and G. Q. Lu, *J. Am. Chem. Soc.*, 2007, **129**, 15650-15654.

11 G. Liu, Y. J. Wang, F. Y. Qiu, L. Li, L. F. Jiao and H. T. Yuan, *J. Mater. Chem.*, 2012, **22**, 22542-22549.

12 Y. Wang, L. Li, C. H. An, Y. J. Wang, C. C. Chen, L. F. Jiao and H. T. Yuan, *Nanoscale*, 2014, **6**, 6684-6691.

13 Y. J. Tan, Y. F. Zhu and L. Q. Li, *Chem. Commun.*, 2015, **51**, 2368-2371.

14 M. Naguib, M. Kurtoglu, V. Presser, J. Lu, J. J. Niu, M. Heon, L. Hultman, Y. Gogotsi and M. W. Barsoum, *Adv. Mater.*, 2011, **23**, 4248-4253.

15 M. Naguib, V. N. Mochalin, M. W. Barsoum and Yury Gogotsi, *Adv. Mater.*, 2014, **26**, 992-1005; J. C. Lei, X. Zhang and Z. Zhou, *Frontiers Phys.*, 2015, **10**, 276-286; X. F. Wang, S. Kajiyama, H. Iinuma, E. Hosono, S. Oro, I. Moriguchi, M. Okubo and A. Yamada, *Nat. Commun.*, 2015, **6**, 6544; Q. K. Hu, D. D. Sun, Q. H. Wu, H. Y. Wang, L. B. Wang, B. Z. Liu, A. G. Zhou and J. L. He, *J. Phys. Chem. A*, 2013, **117**, 14253-14260.

16 M. Naguib, O. Mashtalir, J. Carle, V. Presser, J. Lu, L. Hultman, Y. Gogotsi and M. W. Barsoum, *ACS Nano*, 2012, **6**, 1322-1331; M. R. Lukatskaya, O. Mashtalir, C. E. Ren, Y. Dall´Agnese, P. Rozier, P. L. Taberna, M. Naguib, P. Simon, M. W. Barsoum and Y. Gogotsi, *Science*, 2013, **341**, 1502-1505; M. Ghidiu, M. Naguib, C. Shi, O. Mashtalir, L. M. Pan, B. Zhang, J. Yang, Y. Gogotsi, S. J. L. Billinge and M. W. Barsoum, *Chem. Commun.*, 2014, **50**, 9517-9520.

17 R. R. Shahi, A. Bhatnagar, S. K. Pandey, V. Dixit and O. N. Srivastava, *Int. J. Hydrogen Energy*, 2014, **39**, 14255-14261; G. Liu, Y. J. Wang, L. F. Jiao and H. T. Yuan, *Int. J. Hydrogen Energy*, 2014, **39**, 3822-3829; H. Shao, M. Felderhoff and F. Schüth, *Int. J. Hydrogen Energy*, 2011, **36**, 10828-10833.

18 Y. Dall'Agnese, M. R. Lukatskaya, K.M. Cook, P. L. Taberna, Y. Gogotsi and P. Simon, *Electrochem. Commun.*, 2014, **48**, 118-122.

19 R. B. Rakhi, B. Ahmed, M. N. Hedhili, D. H. Anjum and H.N. Alshareef, *Chem. Mater.*, 2015, **27**, 5314-5323.

20 J. Gu, M. X. Gao, H. G. Pan, Y. F. Liu, B. Li, Y. J. Yang, C. Liang, H. L. Fu and Z. X. Guo, *Energy Environ. Sci.*, 2013, **6**, 847-858; X. Zhang, Y. F. Liu, K. Wang, M. X. Gao and H. G. Pan, *Nano Res.*, 2015, **8**, 533-545.

21 A. A. Voevodin, M. A. Capano, S. J. P. Laube, M. S. Donley and J. S. Zabinski, *Thin Solid Films*, 1997, **298**, 107-115.

22 M. Y. Song, Y. J. Kwak, S. H. Lee, J. Song and D. R. Mumm, *Int. J. Hydrogen Energy*, 2012, **37**, 18133-18139.